

# 000 001 002 003 004 005 006 007 008 009 010 011 012 013 014 015 016 017 018 019 020 021 022 023 024 025 026 027 028 029 030 031 032 033 034 035 036 037 038 039 040 041 042 043 044 045 046 047 048 049 050 051 052 053 REASONING-DRIVEN MULTIMODAL LLMs FOR DOMAIN GENERALIZATION

Anonymous authors

Paper under double-blind review

## ABSTRACT

This paper addresses the domain generalization (DG) problem in deep learning. While most DG methods focus on enforcing visual feature invariance, we leverage the reasoning capability of multimodal large language models (MLLMs) and explore the potential of constructing reasoning chains that derives image categories to achieve more robust predictions under domain shift. To this end, we systematically study the role of reasoning in DG using DomainBed-Reasoning, a newly constructed extension of DomainBed dataset, in which each sample is paired with class-relevant reasoning chains. Our analysis reveals two key challenges: (i) fine-tuning MLLMs with reasoning chains for classification is more challenging than direct label supervision, since the model must optimize complex reasoning sequences before label prediction; and (ii) mismatches in reasoning patterns between supervision signals and fine-tuned MLLMs lead to a trade-off between semantic richness (informative but harder to optimize) and optimization efficiency (easier to optimize but less informative). To address these issues, we propose RD-MLDG (Reasoning-Driven Multimodal LLM for Domain Generalization), a framework with two components: (i) MTCT (Multi-Task Cross-Training), which introduces an additional direct classification pathway to guide reasoning supervision; and (ii) SARR (Self-Aligned Reasoning Regularization), which preserves the semantic richness of reasoning chains while mitigating reasoning-pattern mismatches via iterative self-labeling. Experiments on standard DomainBed datasets (PACS, VLCS, OfficeHome, TerraInc) demonstrate that RD-MLDG achieves state-of-the-art performances, highlighting reasoning as a promising complementary signal for robust out-of-domain generalization.

## 1 INTRODUCTION

In real-world scenarios, deep learning models are often required to generalize reliably to unseen distributions. However, due to domain shift, their performance often degrades substantially when deployed in new environments. To address this issue, Domain Generalization (DG) has emerged as a key research area, aiming to learn representations and prediction functions that transfer well to unseen domains using only source-domain data.

Existing DG approaches generally fall into four categories: invariant representation learning, data augmentation, regularization, and meta-learning. While effective, these methods primarily focus on feature-level invariance and often fail to capture higher-level cross-domain commonalities, limiting their ability to generalize in complex scenarios.

Recently, multi-modal large language models (MLLMs) have made significant progress and demonstrate strong reasoning capabilities. This capability offers a new opportunity for DG: rather than relying solely on invariant feature representations, one could exploit reasoning chains to bridge domain gaps and achieve more robust generalization. By producing structured, class-relevant reasoning chains, we can leverage MLLMs to explicitly decompose a classification task into interpretable and domain invariant steps with strong transferability across domains (Fig. 1). To systematically study the role of reasoning in DG, we leverage GPT-4o to construct DomainBed-Reasoning, an extension of the widely used DomainBed benchmark, where each sample is paired with class-relevant reasoning chains. Specifically, we investigate whether an MLLM fine-tuned with DomainBed-Reasoning can leverage generated reasoning chains to improve domain-generalized predictions.

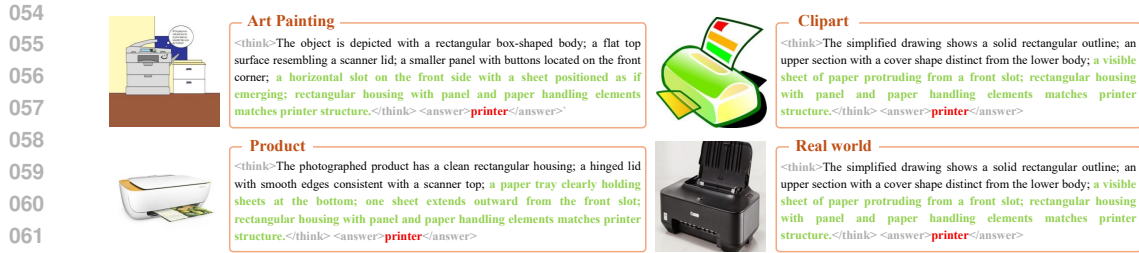


Figure 1: Illustrative examples of the printer in OfficeHome (Art Painting, Clipart, Product, Real World). Although the visual appearance differs substantially, the highlighted green segments of the reasoning chains remain highly consistent, capturing class-relevant cues that are likely to generalize well across domains.

However, our empirical study shows that simply applying reasoning-chain supervision to classification tasks remains challenging. Our analysis reveals two key issues. First, reasoning-chain supervision is inherently difficult to optimize. In contrast to direct label prediction, the model must first fit complex reasoning chains before producing the final label. Second, reasoning chains generated by commercial models and those produced by fine-tuned MLLMs often exhibit distinct reasoning patterns. Commercial-model chains usually contain detailed contextual information that can assist classification, such as descriptions of background, object attributes, or scene conditions. While these chains are semantically rich and potentially informative, they are difficult for the model to optimize. In contrast, self-generated chains from the fine-tuned MLLM tend to be simpler in logic and more label-focused, which makes them easier to fit but less informative for classification. These observations indicate that straightforward reasoning supervision is insufficient and instead call for a more principled integration strategy.

This motivates us to design RD-MLDG (Reasoning-Driven Multimodal LLM for Domain Generalization), the first DG framework that explicitly incorporates class-relevant reasoning chains to enhance out-of-domain performance. RD-MLDG consists of two key components: (i) MTCT (Multi-Task Cross-Training), which jointly optimizes a direct classification pathway and a reasoning-augmented pathway. The direct pathway focuses on standard label prediction, offering a simple and stable training signal. This signal guides the reasoning pathway by preventing it from fitting to overly complex or inconsistent reasoning chains, and instead keeps the supervision focused on the core classification objective; and (ii) Self-Aligned Reasoning Regularization (SARR), which retains informative reasoning chains while mitigating reasoning-pattern mismatches through self-generated supervision. Together, these components enable RD-MLDG to provide a principled way to integrate reasoning into DG for robust generalization.

In summary, our work makes the following contributions:

- We construct DomainBed-Reasoning, an extension of the DomainBed dataset where each sample is paired with class-relevant reasoning chains, enabling systematic evaluation of both classification accuracy and reasoning consistency under domain shift.
- We propose RD-MLDG, the first DG framework that explicitly integrates reasoning by addressing two key challenges: (i) the difficulty of optimizing reasoning-chain supervision, and (ii) mismatches in reasoning patterns between supervision signals and fine-tuned MLLMs.
- We empirically show that RD-MLDG achieves state-of-the-art performance on standard DomainBed benchmarks (PACS, VLCS, OfficeHome, TerraInc), demonstrating the effectiveness of reasoning-based approaches for DG.

## 2 RELATED WORK

**Domain generalization (DG)** has been extensively studied through approaches such as invariant representation learning (e.g., IRM (Arjovsky et al., 2019), CORAL (Sun & Saenko, 2016)), data augmentation (e.g., MixStyle (Zhou et al., 2021), RandConv (Choi et al., 2023)), and learning-based strategies including meta-learning (e.g., MLDG (Li et al., 2018a)), adversarial training (e.g., PAPT (Xu et al., 2025)), and flat-minima regularization (e.g., SWAD (Cha et al., 2021)). Despite their success, these methods primarily operate at the representation level. More recently, CLIP-powered models have advanced DG by providing rich multimodal representations and strong cross-domain transfer. Recent efforts mainly focus on (i) prompt optimization (e.g., CoOp (Zhou et al., 2022b), CoCoOp (Zhou et al., 2022a), KgCoOp (Yao et al., 2023), MaPLe (Khattak et al., 2023))

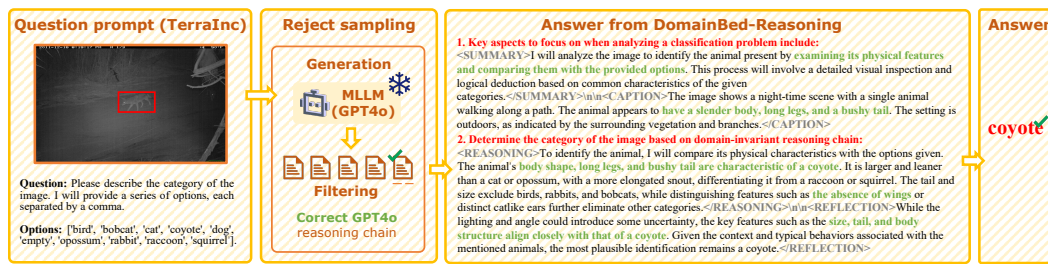


Figure 2: Overview of the DomainBed-Reasoning construction pipeline. GPT-4o generates multi-stage reasoning chains (<SUMMARY>, <CAPTION>, <REASONING>, <REFLECTION>, <CONCLUSION>) without access to ground-truth labels. Multiple candidates are sampled and filtered through rejection sampling to obtain coherent reasoning chains, which form the foundation for analyzing reasoning challenges in DG.

and (ii) leveraging CLIP as a backbone for robustness (e.g., StyLIP (Bose et al., 2024), Prompt-Styler (Cho et al., 2023)). VOLDOGER (Choi et al., 2025) focuses on DG data annotation for vision-language tasks, such as image captioning, visual question answering (VQA), and visual entailment (VE). It alleviates the burden of manual annotation by extending LLM-based annotation techniques and provides a reliable benchmark for evaluating DG in these tasks. While effective, these methods remain confined to feature-level invariance and overlook the reasoning processes that underlie generalizable decision-making. Our work addresses this gap by introducing reasoning as a complementary signal for DG. Specifically, we aim to encourage process-level invariance through class-relevant reasoning chains, which serve as complementary signals to feature-level invariance for improving out-of-domain generalization.

**Multimodal large language models (MLLMs)** have recently emerged as a dominant paradigm for vision–language understanding, achieving strong reasoning and generalization across modalities (e.g., Flamingo (Alayrac et al., 2022), GPT-4V (OpenAI, 2023), Gemini (Team et al., 2023)). Despite these advances, recent studies show that MLLMs underperform their vision encoders (e.g., CLIP (Radford et al., 2021b), EVA-CLIP (Sun et al., 2023)) on fundamental classification benchmarks such as ImageNet, Flowers102, and StanfordCars (Zhang et al., 2024). Existing improvements remain rooted in label-level supervision and fail to capture the explicit reasoning processes required for robust generalization under distribution shift. Our work addresses this gap by leveraging class-relevant reasoning chains and introducing effective training strategies to make reasoning supervision both optimizable and informative, thereby bridging the divide between feature-level alignment and process-level reasoning in MLLMs.

### 3 DOMAINBED-REASONING

A central challenge in studying reasoning for domain generalization (DG) is the lack of benchmarks that explicitly capture reasoning processes. Existing DG datasets provide only input–label pairs, which limits evaluation to feature-level invariance and makes it difficult to assess how reasoning contributes to generalization under domain shift.

To address this gap, we construct **DomainBed-Reasoning**, an extension of the widely used DomainBed benchmark enriched with structured reasoning chains. Specifically, for each image–label pair across four standard DG datasets (PACS, VLCS, OfficeHome, and TerraInc), we employ GPT-4o to generate multi-stage reasoning chains consisting of a <SUMMARY>, <CAPTION>, <REASONING>, <REFLECTION>, and <CONCLUSION>. Compared to the four-step format in LLaVA-CoT (Xu et al., 2024), we introduce an additional reflection stage that prompts the model to self-check intermediate reasoning, which empirically reduces invalid generations and improves stability. Importantly, the ground-truth label is withheld during generation, encouraging reasoning that is grounded in visual evidence rather than rote restatement.

Generating reasoning chains without access to the ground-truth label is non-trivial and may result in incomplete or inconsistent outputs. To improve quality, we adopt a rejection sampling strategy: for each instance, multiple candidate chains are generated, and only those that contain all required components and produce a coherent conclusion are retained. An overview of this construction pipeline is illustrated in Fig. 2. The resulting dataset pairs classification labels with independently generated

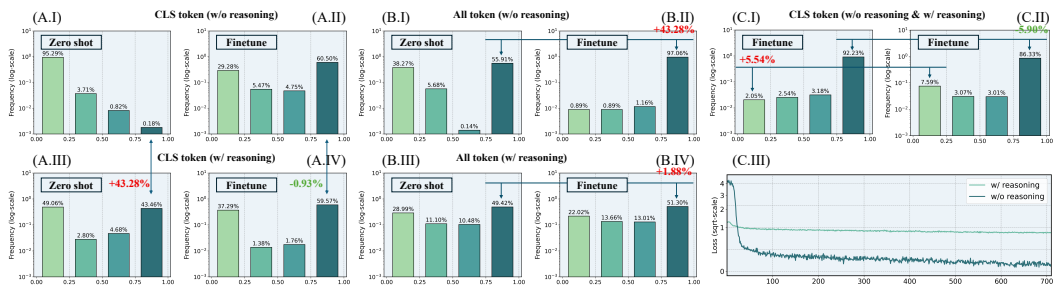


Figure 3: Illustration of Challenge 1 (see Sec. 4.1). (A) Classification token probabilities on target-domain test data under zero-shot and SFT, with and without reasoning; (B) Probability distributions of all tokens on source-domain training data under zero-shot and SFT; (C) Training dynamics: (I-II) classification token probabilities on source-domain training data after SFT; (III) loss curves comparing reasoning-based and no-thinking SFT.

reasoning chains, enabling evaluation under domain shift. DomainBed-Reasoning thus provides a standardized extension of DomainBed for studying reasoning-based domain generalization, serving as a foundation to analyze how reasoning supervision affects out-of-domain performance (Sec. 4).

## 4 CHALLENGES OF REASONING CHAIN IN DG

DomainBed-Reasoning provides a basis to analyze the role of reasoning in DG, and our study indicates that using reasoning-chain supervision alone for classification is challenging, especially under supervised fine-tuning. We identify two main issues: (i) the difficulty of optimizing reasoning-chain supervision under domain shift (Sec. 4.1), and (ii) mismatches in reasoning patterns between supervision signals and fine-tuned MLLMs (Sec. 4.2). These challenges highlight the gap between the potential of reasoning and its current limitations in DG, motivating the RD-MLDG framework introduced in the next section.

### 4.1 OPTIMIZATION GAP IN REASONING-CHAIN SUPERVISION

**Research Question.** *Does directly distilling class-relevant reasoning chains into MLLMs improve domain generalization in classification?*

**Experiment Setting.** As a case study, we conduct experiments on the TerraInc dataset (Beery et al., 2018), which contains 10 categories of wild animals across diverse camera locations, with domain shifts arising from viewpoint and background variations. We use InternVL3-8B (Chen et al., 2024) as the base model and compare two training regimes: (i) no-thinking (Li et al., 2025), where the model takes the image and input question (e.g., “What type of object is in this photo? Choose from the following options:”) and directly predicts the label, and (ii) reasoning-chain supervision using DomainBed-Reasoning, where the same inputs are paired with multi-stage reasoning chains. Both regimes are evaluated under zero-shot prompting and supervised fine-tuning (SFT). To assess their behavior, we analyze token probability distributions and training dynamics (Fig. 3).

**Observation.** First, in the zero-shot setting, adding reasoning improves classification performance under domain shift: InternVL3-8B shows a **+43.28%<sub>p</sub>** increase in ground-truth token probability compared to no-thinking predictions (Fig. 3.A, I vs III). Second, this benefit does not persist under supervised fine-tuning (SFT): reasoning-chain supervision yields slightly lower accuracy (**-0.93%<sub>p</sub>**) than direct label supervision (Fig. 3.A, II vs IV). Third, token-level distributions further highlight this optimization gap. No-thinking SFT shifts a large proportion of tokens from low to high probability (**+43.38%<sub>p</sub>**) (Fig. 3.B, I vs II), whereas reasoning-chain SFT produces only a marginal gain (**+1.88%<sub>p</sub>**) (Fig. 3.B, III vs IV). Training dynamics show a similar trend: no-thinking SFT fits classification tokens more effectively (92.23% vs 86.33% above the 75% confidence threshold), while reasoning-based SFT retains more low-probability samples (7.59% vs 2.05% below 25%) (Fig. 3.C.I-II). Finally, loss curves (Fig. 3.C.III) suggest that reasoning-based supervision converges more slowly, indicating that reasoning-chain supervision is harder to optimize than direct label prediction.

**Insight.** These results suggest that zero-shot reasoning can enhance out-of-domain generalization, but directly distilling reasoning chains during supervised fine-tuning is less effective than using label

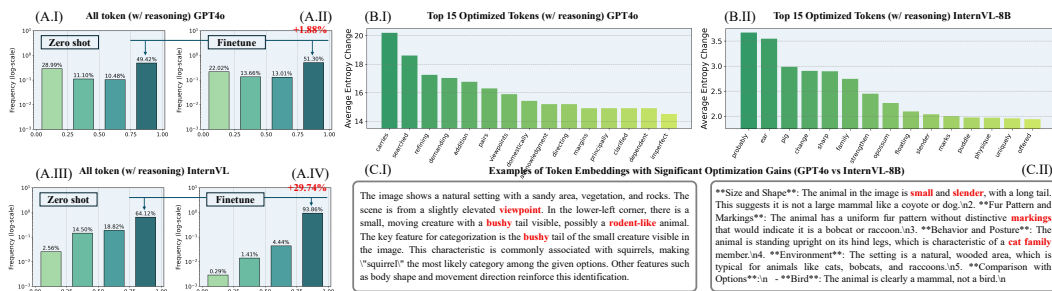


Figure 4: Illustration of Challenge 2 (see Sec. 4.2). (A) Token probability distributions on source-domain training data under zero-shot and fine-tuned settings: GPT-4o reasoning (A.I, A.II) vs InternVL3-8B reasoning (A.III, A.IV). (B) Top-15 tokens with the largest entropy reduction during optimization, highlighting differences between GPT-4o (B.I) and InternVL3-8B (B.II). (C) Qualitative examples corresponding to (B.I) and (B.II), with tokens receiving the strongest optimization gains highlighted in red.

supervision alone. A key difficulty is that reasoning-chain supervision requires optimizing an intermediate step before predicting the final label, which slows convergence and reduces its effectiveness for classification learning. This limitation motivates the introduction of a direct classification pathway to guide reasoning supervision, making reasoning signals more effective for classification.

## 4.2 MISMATCHES IN REASONING PATTERNS ACROSS SOURCES

**Research Question.** *How do mismatches in reasoning patterns across different reasoning sources influence the supervision signals and optimization behavior of models?*

**Experiment Setting.** We use the same dataset and base model as in Sec. 4.1. To study mismatches in reasoning patterns, we compare fine-tuning with reasoning chains generated by a large MLLM (GPT-4o) versus those produced by the target model itself (InternVL3-8B). We then analyze how these different supervision sources affect token-level optimization by (i) comparing probability distributions of all tokens in zero-shot and fine-tuned settings, and (ii) examining the top-15 tokens with the largest entropy reduction (Fig. 4).

**Observation.** Fig. 4 shows how mismatches in reasoning patterns affect token-level optimization during fine-tuning. First, comparing token probability distributions (Fig. 4.A), reasoning chains generated by GPT-4o contain richer contextual descriptions (e.g., background, viewpoint), but fine-tuning with them yields only a marginal token shift (**+1.88%<sub>p</sub>**, A.I vs A.II). In contrast, when using reasoning chains generated by InternVL3-8B itself, fine-tuning produces a much larger token shift (**+29.74%<sub>p</sub>**, A.III vs A.IV), indicating that these chains are easier for the model to fit. Second, the entropy-based analysis (Fig. 4.B) reflects the same trend: GPT-4o reasoning exposes the model to fine-grained descriptive details that may be informative but are less directly aligned with classification, whereas self-generated reasoning emphasizes category-related tokens (e.g., ‘cat family’, ‘bird’). Finally, qualitative examples (Fig. 4.C) illustrate these reasoning styles: GPT-4o produces longer, context-rich chains, while InternVL3-8B generates shorter, label-focused explanations. Tokens highlighted in red denote those with the largest entropy reduction. Together, these observations suggest a trade-off: large-model reasoning provides richer but harder-to-optimize signals, while self-generated reasoning provides simpler cues that focus more directly on the category label.

**Insight.** These results suggest that mismatches between large-model reasoning (e.g., GPT-4o) and self-generated reasoning (InternVL3-8B) create a trade-off between contextual detail and ease of optimization. Large-model chains provide richer descriptions but include complex, high-entropy tokens that are harder to optimize, while self-generated chains are easier to fit but focus mainly on the category label and its immediate features. This trade-off may reduce the effectiveness of direct reasoning-chain supervision, motivating methods that preserve useful semantic detail while making reasoning signals easier to optimize.

## 5 METHOD

**Problem Definition.** Let  $\mathcal{X}$  denote the input space and  $\mathcal{Y}$  the label space. In domain generalization (DG), we assume access to  $N_s$  labeled source domains  $\hat{\mathcal{D}}^S = \{\hat{\mathcal{D}}_m^S\}_{m=1}^{N_s}$ , where each  $\hat{\mathcal{D}}_m^S$  is an

270 empirical distribution over  $\mathcal{X} \times \mathcal{Y}$  drawn from a distinct but related environment. For the  $m$ -th  
 271 source domain with  $N_m^s$  labeled samples, we write  $\hat{\mathcal{D}}_m^S = \{(\mathbf{x}_i, y_i)\}_{i=1}^{N_m^s}$ , where  $\mathbf{x}_i \in \mathcal{X}$  denotes an  
 272 input image and  $y_i \in \mathcal{Y}$  its corresponding label. The goal of DG is to learn a model that generalizes  
 273 to unseen target domains at test time, without access to any target data during training. The unseen  
 274 target set is denoted as  $\hat{\mathcal{D}}^T = \{\hat{\mathcal{D}}_m^T\}_{m=1}^{N_t}$ , where each  $\hat{\mathcal{D}}_m^T$  is a distribution over  $\mathcal{X}$  corresponding to  
 275 an unseen domain, with  $\hat{\mathcal{D}}_m^T \notin \hat{\mathcal{D}}^S$  for all  $m$ .  
 276

277 **Overall Framework of our Method.** To address the challenges identified in Sec. 4, we propose  
 278 RD-MLDG (Reasoning-Driven Multimodal LLM for Domain Generalization), a framework that in-  
 279 tegrates reasoning into DG. RD-MLDG has two modules: (i) Multi-Task Cross-Training (MTCT),  
 280 which jointly optimizes a direct classification pathway and reasoning-chain supervision, so that  
 281 the classification objective provides a stable signal to guide reasoning optimization, addressing the  
 282 optimization difficulty in Challenge 1 (Sec. 4.1); and (ii) Self-Aligned Reasoning Regularization  
 283 (SARR), which leverages self-labeling to produce reasoning chains consistent with the model’s own  
 284 reasoning style, thereby retaining useful contextual detail while reducing reasoning-pattern mis-  
 285 matches, addressing Challenge 2 (Sec. 4.2). Together, these modules make reasoning supervision  
 286 more optimizable and informative, offering a structured way to incorporate reasoning into DG for  
 287 improved out-of-domain performance.  
 288

### 288 5.1 MULTI-TASK CROSS-TRAINING

290 Motivated by the difficulty of optimizing reasoning-chain supervision observed in Challenge 1,  
 291 Multi-Task Cross-Training (MTCT) trains the model to jointly optimize reasoning-chain supervision  
 292 with a direct classification pathway. The key idea is that classification supervision serves as a simple  
 293 and stable anchor objective, which guides reasoning optimization and helps alleviate the difficulty  
 294 of fitting intermediate reasoning steps before predicting the final label. Concretely, for each training  
 295 image  $\mathbf{x}_i$ , we construct two prompts: (i) a **reasoning prompt** from DomainBed-Reasoning with its  
 296 corresponding class-relevant reasoning chain  $\mathbf{r}_i$ , and (ii) a **classification prompt** (no-thinking) —  
 297 “What type of object is in this photo? Choose from the following options.” — where the model  
 298 selects from a candidate label list and the ground-truth label  $y_i$  is used as the supervision signal. We  
 299 denote these instruction templates as  $\mathbf{q}_{\text{reason}}$  and  $\mathbf{q}_{\text{cls}}$ , respectively.  
 300

301 We fine-tune the base multimodal large language model (MLLM) by inserting LoRA adapters  
 302 into both the vision encoder and the language decoder, enabling parameter-efficient supervised  
 303 fine-tuning (SFT) without updating all parameters. Given a batch  $\{(\mathbf{x}_i, y_i, \mathbf{r}_i)\}_{i=1}^B$ , where  $\mathbf{r}_i =$   
 304  $(r_{i,1}, \dots, r_{i,T_i})$  is the class-relevant reasoning chain for  $\mathbf{x}_i$  and  $\mathbf{r}_{i,< t} = (r_{i,1}, \dots, r_{i,t-1})$  denotes  
 305 the prefix sequence before predicting token  $r_{i,t}$ , the MTCT loss can be defined as follows:  
 306

$$307 \mathcal{L}_{\text{MTCT}} = \frac{1}{B} \sum_{i=1}^B \left[ -\log p_{\theta}(y_i \mid \mathbf{x}_i, \mathbf{q}_{\text{cls}}) - \frac{1}{T_i} \sum_{t=1}^{T_i} \log p_{\theta}(r_{i,t} \mid \mathbf{r}_{i,< t}, \mathbf{x}_i, \mathbf{q}_{\text{reason}}) \right], \quad (1)$$

308 where  $T_i$  denotes the length (number of tokens) of the reasoning chain  $\mathbf{r}_i$ , and is used to normalize  
 309 the generation loss so that longer chains do not dominate the gradients.  
 310

311 This formulation directly addresses the optimization difficulty identified in Sec. 4.1, making reasoning  
 312 supervision more stable and effective for domain generalization.  
 313

### 313 5.2 SELF-ALIGNED REASONING REGULARIZATION

315 After the first stage MTCT training, the model has already been trained with reasoning chains dis-  
 316 tillied from large MLLMs (e.g., GPT-4o). However, directly relying on this supervision can be chal-  
 317 lenging due to reasoning-pattern mismatches, as discussed in Sec. 4.2. To mitigate this issue, we  
 318 introduce Self-Aligned Reasoning Regularization (SARR), a soft self-labeling procedure. Specif-  
 319 ically, the model generates its own reasoning under the instruction  $\mathbf{q}_{\text{reason}}$ . From each output, we  
 320 extract the predicted conclusion enclosed between `<CONCLUSION>` and `</CONCLUSION>` and  
 321 compare it with the ground-truth label  $y_i$ . Only reasoning chains with correct final conclusions are  
 322 retained and used as refined supervision signals.  
 323

These retained reasoning chains are then combined with the classification prompt  $\mathbf{q}_{\text{cls}}$  as part of the  
 MTCT fine-tuning process. In each round of SARR, the reasoning chains, initially sourced from

324  
 325 Table 1: Multi-source DG results (%) on DomainBed benchmark datasets. The best performances in  
 326 comparisons are highlighted in **bold** and the second-best ones are marked with underlines.

Method	Venue	PACS	VLCS	OfficeHome	TerraInc	Avg.
<i>ResNet-50 Based Method.</i>						
CORAL (Sun & Saenko, 2016)	ICCV'16	86.20 $\pm$ 0.30	78.80 $\pm$ 0.60	68.70 $\pm$ 0.30	47.60 $\pm$ 1.00	70.33
MLDG (Li et al., 2018a)	AAAI'18	84.90 $\pm$ 1.00	77.20 $\pm$ 0.40	66.80 $\pm$ 0.60	47.70 $\pm$ 0.90	69.15
Mixstyle (Zhou et al., 2021)	ICLR'21	85.20 $\pm$ 0.30	77.90 $\pm$ 0.50	60.40 $\pm$ 0.20	44.00 $\pm$ 0.70	66.88
DomainDrop (Guo et al., 2023a)	ICCV'23	87.90 $\pm$ 0.30	79.80 $\pm$ 0.30	68.70 $\pm$ 0.10	51.50 $\pm$ 0.40	71.98
SMOS (Luo et al., 2024)	CVPR'24	89.40 $\pm$ 0.30	79.80 $\pm$ 0.10	71.60 $\pm$ 0.10	55.40 $\pm$ 0.40	74.05
RES (Huang et al., 2025)	ECCV'24	90.00 $\pm$ 0.30	79.80 $\pm$ 0.20	71.80 $\pm$ 0.30	51.40 $\pm$ 0.60	73.25
GGA (Ballas & Diou, 2025)	CVPR'25	87.30 $\pm$ 0.40	79.90 $\pm$ 0.40	68.50 $\pm$ 0.20	50.60 $\pm$ 0.10	71.58
<i>VIT-B/16 Based Method.</i>						
SWAD (Cha et al., 2021)	NIPS'21	91.30 $\pm$ 0.10	79.40 $\pm$ 0.40	76.90 $\pm$ 0.10	45.40 $\pm$ 0.50	73.25
CLIP (Radford et al., 2021a)	-	96.20 $\pm$ 0.10	81.70 $\pm$ 0.10	82.00 $\pm$ 0.10	33.40 $\pm$ 0.10	73.33
CoOp (Zhou et al., 2022b)	IJCV'22	96.20 $\pm$ 0.10	77.60 $\pm$ 0.20	83.90 $\pm$ 0.10	48.80 $\pm$ 0.10	76.63
MaPLe (Khattak et al., 2023)	CVPR'23	96.50 $\pm$ 0.20	82.20 $\pm$ 0.20	83.40 $\pm$ 0.00	50.20 $\pm$ 0.90	78.08
SIMPLE <sup>+</sup> (Li et al., 2023b)	ICLR'23	<b>99.00</b> $\pm$ 0.10	82.70 $\pm$ 0.40	87.70 $\pm$ 0.40	59.00 $\pm$ 0.60	82.10
VL2V-SD (Addepalli et al., 2024)	CVPR'24	95.67 $\pm$ 0.56	82.67 $\pm$ 0.36	85.44 $\pm$ 0.27	41.18 $\pm$ 0.74	76.24
CLIP-LoRA Zanella & Ben Ayed (2024)	CVPR'24	97.10 $\pm$ 0.00	83.10 $\pm$ 0.00	83.90 $\pm$ 0.00	55.70 $\pm$ 0.00	79.95
SPG (Bai et al., 2025)	ECCV'24	97.00 $\pm$ 0.50	82.40 $\pm$ 0.40	83.60 $\pm$ 0.40	50.20 $\pm$ 1.20	78.30
DGCLDTP (Wen et al., 2025)	CVPR'25	97.03 $\pm$ 0.00	84.79 $\pm$ 0.00	87.65 $\pm$ 0.00	<b>63.27</b> $\pm$ 0.00	83.19
<i>MLM Based Method.</i>						
GPT4o (OpenAI, 2023)	-	97.83 $\pm$ 0.00	85.41 $\pm$ 0.00	90.12 $\pm$ 0.00	60.49 $\pm$ 0.00	<b>83.46</b>
InternVL3-8B (Zhu et al., 2025)	-	96.26 $\pm$ 0.10	<u>85.67</u> $\pm$ 0.10	85.10 $\pm$ 0.10	46.84 $\pm$ 0.20	78.47
InternVL3-8B + RD-MLDG (Ours)	-	98.13 $\pm$ 0.10	<b>87.03</b> $\pm$ 0.10	<u>91.73</u> $\pm$ 0.10	<b>70.65</b> $\pm$ 0.10	<b>86.89</b>

346  
 347 **GPT-4o** in the first stage, are replaced by self-generated reasoning chains in later stages. The training  
 348 objective for each round of SARR remains the same as MTCT, where the model is fine-tuned  
 349 using both reasoning chains and the classification prompt. Given a batch with self-generated reasoning  
 350 chains  $(\mathbf{x}_i, y_i, \hat{\mathbf{r}}_i)_{i=1}^{B'}$ , where  $\hat{\mathbf{r}}_i$  denotes a reasoning chain retained because its final conclusion  
 351 matches the ground-truth label, the loss in SARR for each round can be defined as:

$$\mathcal{L}_{\text{SARR}} = \frac{1}{B'} \sum_{i=1}^{B'} \left[ -\log p_{\theta}(y_i \mid \mathbf{x}_i, \mathbf{q}_{\text{cls}}) - \frac{1}{T_i} \sum_{t=1}^{T_i} \log p_{\theta}(\hat{\mathbf{r}}_{i,t} \mid \hat{\mathbf{r}}_{i,< t}, \mathbf{x}_i, \mathbf{q}_{\text{reason}}) \right]. \quad (2)$$

352 This self-labeling procedure can be repeated for  $N$  rounds. In each round, the model is trained  
 353 with both classification ( $\mathbf{q}_{\text{cls}}$ ) and reasoning ( $\mathbf{q}_{\text{reason}}$ ) prompts, generates reasoning chains for the  
 354 source domain training data, and keeps only those whose final conclusions match the ground-truth  
 355 label. The model is then fine-tuned again with these reasoning-classification pairs. Through this  
 356 iterative refinement, the supervision becomes both informative and easier to fit, helping mitigate the  
 357 reasoning-pattern mismatches identified in Sec. 4.2.

## 6 EXPERIMENTS

364  
 365 **Datasets and Evaluation Protocols.** We adopt four widely used benchmarks for evaluation:  
 366 PACS (Li et al., 2017) (4 domains, 9,991 samples, 7 classes), VLCS (Li et al., 2017) (4 domains,  
 367 10,729 samples, 5 classes), OfficeHome (Venkateswara et al., 2017) (4 domains, 15,588 samples,  
 368 65 classes), and TerraInc (Beery et al., 2018) (4 domains, 24,788 samples, 10 classes).

369 For each dataset, we use the extended DomainBed-Reasoning version, where each image-label  
 370 pair is paired with structured reasoning chains generated by GPT-4o (see Sec. 3). We evaluate  
 371 classification under domain shift using the standard DomainBed leave-one-domain-out protocol and  
 372 report the average test accuracy (Avg-acc) across all target domains. To reduce variance, results are  
 373 averaged over three runs with different random seeds.

374 **Implementation Details.** We follow the supervised fine-tuning (SFT) procedure described in Sec. 5.  
 375 Each training stage runs for 3 epochs with a batch size of 128 and a learning rate of 5e-4. We use  
 376 AdamW as the optimizer. LoRA adapters (rank 8) are applied to both the vision encoder and the  
 377 language decoder for parameter-efficient fine-tuning. For SARR (Sec. 5.2), we set the number of  
 378 self-labeling rounds to  $N = 3$ . All experiments are conducted on 4 NVIDIA A100 GPUs (80GB).

378

379

Table 2: Ablation study on each component on OfficeHome and TerraIncognita dataset.

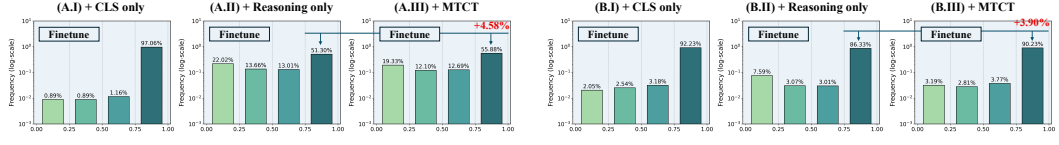
380

381

Idx	Method	Art	Clipart	OfficeHome			TerraIncognita			
				Product	Real	Avg.	L100	L38	L43	L46
1	GPT-4o	87.10	85.36	95.20	92.82	90.12	67.28	59.71	64.47	50.49
2	<b>InternVL3-2B</b>	<b>3.79</b>	<b>3.64</b>	<b>2.70</b>	<b>3.49</b>	<b>3.41</b>	<b>0.16</b>	<b>0.25</b>	<b>0.15</b>	<b>0.33</b>
3	+ CLS only	88.59	81.49	94.46	92.10	89.16	75.26	64.66	69.98	55.99
4	+ Reasoning only (Baseline)	87.03	82.13	93.77	91.45	88.60	74.79	61.26	69.40	58.56
5	+ MTCT	<b>89.00</b>	<b>83.71</b>	<b>95.49</b>	<b>93.53</b>	<b>90.43</b> ( $\uparrow 1.83\%$ )	<b>77.82</b>	<b>65.03</b>	<b>72.71</b>	<b>59.41</b>
6	+ SARR	<b>88.30</b>	<b>82.54</b>	<b>95.29</b>	<b>93.07</b>	<b>89.80</b> ( $\uparrow 1.20\%$ )	<b>75.83</b>	<b>62.08</b>	<b>69.51</b>	<b>59.27</b>
7	+ MTCT + SARR	<b>90.13</b>	<b>84.57</b>	<b>96.00</b>	<b>93.62</b>	<b>91.08</b> ( $\uparrow 2.48\%$ )	<b>82.43</b>	<b>66.54</b>	<b>73.62</b>	<b>61.15</b>
8	<b>InternVL3-8B</b>	<b>81.95</b>	<b>78.26</b>	<b>91.91</b>	<b>88.27</b>	<b>85.10</b>	<b>61.84</b>	<b>41.27</b>	<b>45.60</b>	<b>38.66</b>
9	+ CLS only	87.27	82.59	95.11	92.59	89.39	72.80	65.64	69.70	58.62
10	+ Reasoning only (Baseline)	86.59	82.45	94.33	91.66	88.76	74.42	60.39	68.21	55.21
11	+ MTCT	<b>89.33</b>	<b>83.53</b>	<b>95.79</b>	<b>93.67</b>	<b>90.58</b> ( $\uparrow 1.81\%$ )	<b>76.78</b>	<b>60.55</b>	<b>71.94</b>	<b>59.47</b>
12	+ SARR	<b>90.89</b>	<b>83.34</b>	<b>95.95</b>	<b>93.44</b>	<b>90.91</b> ( $\uparrow 2.14\%$ )	<b>74.97</b>	<b>60.96</b>	<b>68.28</b>	<b>56.96</b>
13	+ MTCT + SARR	<b>91.72</b>	<b>85.14</b>	<b>96.25</b>	<b>93.81</b>	<b>91.73</b> ( $\uparrow 2.97\%$ )	<b>81.74</b>	<b>66.12</b>	<b>73.38</b>	<b>61.36</b>
										<b>70.65</b> ( $\uparrow 6.09\%$ )

386

387



396

397

Figure 5: Analysis of MTCT (Sec. 5.1). Probability distributions on TerraInc source domain training data under direct label prediction, reasoning-only SFT, and MTCT SFT: (A) all tokens and (B) class tokens.

398

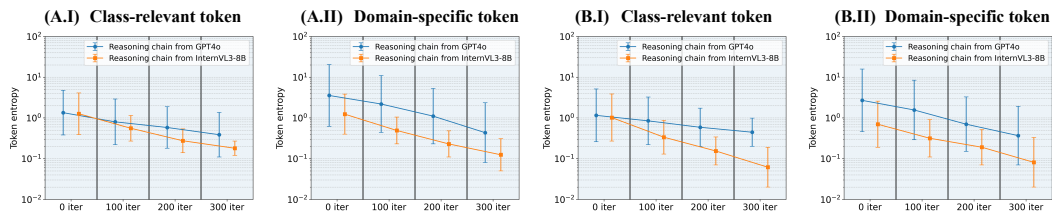
399

## 6.1 RESULTS ON MULTIPLE DOMAIN GENERALIZATION

400

To demonstrate the effectiveness of our proposed RD-MLDG, we compare it with representative SOTA methods (Tab. 1). Built on InternVL3-8B, RD-MLDG achieves the best average accuracy of 86.89%, surpassing a strong commercial MLLM (GPT-4o, 83.46%) and competitive CLIP/ViT approaches (e.g., DGCLDTP, 83.19%). Per-dataset, RD-MLDG attains new best results on VLCS (87.03%), OfficeHome (91.73%), and TerraInc (70.65%), while remaining highly competitive on PACS (98.13%). To sum up, our proposed method has two main advantages: (1) Compared to feature-level invariant representation learning, RD-MLDG leverages class-relevant reasoning chains, which are explicitly observable and understandable by humans, rather than relying on latent feature representations that are difficult to interpret. (2) Through an efficient two-stage supervised fine-tuning procedure, our method avoids the need for complex training strategies while substantially enhancing the classification ability of the underlying MLLM under domain shift.

411



419

Figure 6: Analysis of SARR (see Sec. 5.2) from token entropy on TerraInc (A) and OfficeHome (B). We track the entropy of selected **class-relevant** (A.I & B.I) and **domain-specific** tokens (A.II & B.II) across fine-tuning iterations, with vertical bars denoting variation across samples. Blue curves correspond to fitting GPT-4o reasoning chains, and orange curves to InternVL3-8B self-generated reasoning chains.

423

## 6.2 ABLATION STUDY

425

To further evaluate the effectiveness of each component, we conduct ablations using InternVL3-2B and InternVL3-8B on OfficeHome and TerraInc; results are shown in Tab. 2. The very low zero-shot result of InternVL3-2B (2<sup>nd</sup> row) is due to its **limited instruction-following** ability, but fine-tuning with reasoning chains supervision (4<sup>th</sup> row) quickly recovers strong baselines.

430

431

**Effectiveness of Multi-Task Cross-Training.** On both OfficeHome and TerraInc, direct label prediction outperforms reasoning-chain supervision: +0.56%p and +0.47%p on InternVL3-2B (3<sup>rd</sup> vs. 4<sup>th</sup> rows), and +0.63%p and +2.13%p on InternVL3-8B (9<sup>th</sup> vs. 10<sup>th</sup> rows), supporting the obser-

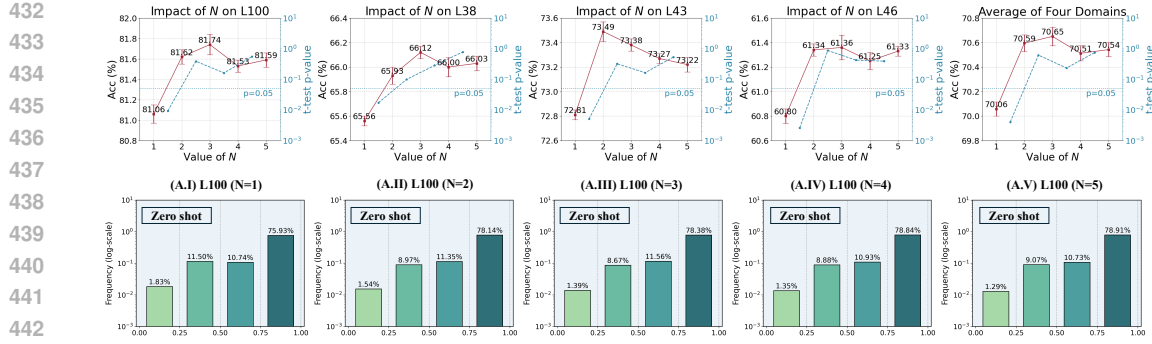


Figure 7: Impact of the number of self-labeling rounds  $N$  in SARR (Sec. 5.2) on TerraInc using InternVL3-8B. Top: classification accuracy on four domains (L100, L38, L43, L46) and their average, with paired  $t$ -test  $p$ -values for adjacent  $N$  shown on the right axis (reference line at  $p = 0.05$ ). Bottom: zero-shot token probability distributions (log-scale) on L100, using supervision data from each self-labeling round.

vation from Challenge 1 that reasoning-only supervision is less effective for classification. Relative to the reasoning-only baseline, MTCT yields additional improvements of +1.83%p and +2.74%p on InternVL3-2B (4<sup>th</sup> vs. 5<sup>th</sup> rows), and +1.81%p and +2.63%p on InternVL3-8B (10<sup>th</sup> vs. 11<sup>th</sup> rows), supporting that the direct classification pathway provides a stable signal that helps reasoning supervision contribute more effectively. Moreover, when combined with SARR, MTCT brings further gains of +1.28%p and +4.27%p on InternVL3-2B (6<sup>th</sup> vs. 7<sup>th</sup> rows), and +0.83%p and +5.36%p on InternVL3-8B (12<sup>th</sup> vs. 13<sup>th</sup> rows), reinforcing its role in guiding reasoning optimization.

Fig. 5 provides further evidence from the token-probability perspective. In Fig. 5.A, the **all-token distributions** show that MTCT still struggles to fully fit the semantically rich reasoning chains generated by GPT-4o, with 19.33% of tokens remaining at low probability after fine-tuning. By contrast, Fig. 5.B highlights consistent improvements in the **class-token distributions**: the proportion of high-confidence class tokens ( $>0.75$ ) rises from 86.33% to 90.23%, while the share of low-confidence class tokens drops from 7.59% to 3.19%. These results indicate that MTCT does not substantially enhance the modeling of all reasoning details, but it does strengthen the fitting of class tokens, which directly supports the classification objective.

**Effectiveness of Self-Aligned Reasoning Regularization.** On OfficeHome and TerraInc, SARR improves accuracy over direct reasoning-chain supervision by +1.20%p and +0.67%p on InternVL3-2B (4<sup>th</sup> vs. 6<sup>th</sup> rows), and by +2.14% and +0.73% on InternVL3-8B (10<sup>th</sup> vs. 12<sup>th</sup> rows). When combined with MTCT, it brings further gains of +0.65%p and +2.20%p on InternVL3-2B (5<sup>th</sup> vs. 7<sup>th</sup> rows), and +1.15%p and +3.46%p on InternVL3-8B (11<sup>th</sup> vs. 13<sup>th</sup> rows). These results support the insight from Challenge 2: self-labeled reasoning retains class-relevant information from large-model supervision while producing signals that the model can fit more effectively.

Fig. 6.A reports token-entropy dynamics on TerraInc. We note two key observations. First, for **class-relevant tokens** (e.g., mark, floating), GPT-4o and InternVL3-8B reasoning chains start with similar entropy in the zero-shot stage, but as fine-tuning proceeds, entropy decreases faster for InternVL3-8B, showing that SARR shifts supervision toward signals the model can fit more readily. Second, for **domain-specific tokens** (e.g., demanding, viewpoint), GPT-4o reasoning chains have higher initial entropy than self-generated chains, reflecting richer but harder-to-fit details; with SARR, the model reduces fitting pressure on these tokens and instead focuses on class-relevant ones. This reallocation of optimization effort helps explain the accuracy gains of SARR. Results on OfficeHome (Fig. 6.B) show the same trend.

### 6.3 PARAMETER ANALYSIS

We further analyze how the number of self-labeling rounds  $N$  affects performance on TerraInc (Fig. 7, top). We report  $p$ -values from paired  $t$ -tests, where runs with the same random seed are compared across adjacent  $N$  settings. Accuracy shows a small but statistically significant improvement from 70.06% at  $N = 1$  to 70.59% at  $N = 2$  ( $p < 0.01$ ). At  $N = 3$ , accuracy reaches 70.65%, but the improvement over  $N = 2$  is not statistically significant ( $p \approx 0.07$ ). For  $N > 3$ , accuracy remains stable between 70.50% and 70.60% with  $p$ -values above 0.1.

We also examine the zero-shot token-probability distributions across different self-labeling rounds (Fig. 7, bottom). From  $N = 1$  to  $N = 2$ , the proportion of high-confidence tokens increases (2.27%) while low-confidence tokens decrease (0.29%), indicating a clearer supervision signal. For  $N \geq 3$ , the probability distribution remains nearly unchanged, showing that self-labeling converges within the first few rounds. We therefore set  $N = 3$  in our experiments.

## 7 CONCLUSION

This work investigated how reasoning can contribute to domain generalization and identified two key challenges: optimization difficulty and reasoning-pattern mismatch. To address these issues, we proposed RD-MLDG, which integrates class-relevant reasoning chains with label supervision through MTCT and SARR. Experiments on DomainBed show that RD-MLDG achieves the best reported performance among strong baselines.

## REFERENCES

Sravanti Addepalli, Ashish Ramayee Asokan, Lakshay Sharma, and R Venkatesh Babu. Leveraging vision-language models for improving domain generalization in image classification. In *Proceedings of the IEEE/CVF Conference on Computer Vision and Pattern Recognition*, pp. 23922–23932, 2024.

Jean-Baptiste Alayrac, Jeff Donahue, Pauline Luc, Antoine Miech, Iain Barr, Yana Hasson, Arthur Mensch, Katherine Millican, Malcolm Reynolds, et al. Flamingo: a visual language model for few-shot learning. In *NeurIPS*, 2022.

Martin Arjovsky, Léon Bottou, Ishaan Gulrajani, and David Lopez-Paz. Invariant risk minimization. *arXiv preprint arXiv:1907.02893*, 2019.

Shuanghao Bai, Yuedi Zhang, Wanqi Zhou, Zhirong Luan, and Badong Chen. Soft prompt generation for domain generalization. In *European Conference on Computer Vision*, pp. 434–450. Springer, 2025.

Aristotelis Ballas and Christos Diou. Gradient-guided annealing for domain generalization. In *Proceedings of the Computer Vision and Pattern Recognition Conference*, pp. 20558–20568, 2025.

Sara Beery, Grant Van Horn, and Pietro Perona. Recognition in terra incognita. In *Proceedings of the European conference on computer vision (ECCV)*, pp. 456–473, 2018.

Gilles Blanchard, Aniket Anand Deshmukh, Urun Dogan, Gyemin Lee, and Clayton Scott. Domain generalization by marginal transfer learning. *Journal of machine learning research*, 22(2):1–55, 2021.

Shirsha Bose, Ankit Jha, Enrico Fini, Mainak Singha, Elisa Ricci, and Biplab Banerjee. Stylip: Multi-scale style-conditioned prompt learning for clip-based domain generalization. In *Proceedings of the IEEE/CVF Winter Conference on Applications of Computer Vision*, pp. 5542–5552, 2024.

Junbum Cha, Sanghyuk Chun, Kyungjae Lee, Han-Cheol Cho, Seunghyun Park, Yunsung Lee, and Sungrae Park. Swad: Domain generalization by seeking flat minima. *Advances in Neural Information Processing Systems*, 34:22405–22418, 2021.

Liang Chen, Yong Zhang, Yibing Song, Ying Shan, and Lingqiao Liu. Improved test-time adaptation for domain generalization. In *Proceedings of the IEEE/CVF Conference on Computer Vision and Pattern Recognition*, pp. 24172–24182, 2023a.

Liang Chen, Yong Zhang, Yibing Song, Anton Van Den Hengel, and Lingqiao Liu. Domain generalization via rationale invariance. In *Proceedings of the IEEE/CVF International Conference on Computer Vision*, pp. 1751–1760, 2023b.

540 Zhe Chen, Jiannan Wu, Wenhui Wang, Weijie Su, Guo Chen, Sen Xing, Muyan Zhong, Qinglong  
 541 Zhang, Xizhou Zhu, Lewei Lu, et al. Internvl: Scaling up vision foundation models and aligning  
 542 for generic visual-linguistic tasks. In *Proceedings of the IEEE/CVF Conference on Computer  
 543 Vision and Pattern Recognition*, pp. 24185–24198, 2024.

544 Junhyeong Cho, Gilhyun Nam, Sungyeon Kim, Hunmin Yang, and Suha Kwak. Promptstyler:  
 545 Prompt-driven style generation for source-free domain generalization. In *Proceedings of the  
 546 IEEE/CVF International Conference on Computer Vision*, pp. 15702–15712, 2023.

547 Juhwan Choi, Junehyoung Kwon, JungMin Yun, Seunguk Yu, and YoungBin Kim. Voldoger:  
 548 Llm-assisted datasets for domain generalization in vision-language tasks. In *Proceedings of the  
 549 IEEE/CVF International Conference on Computer Vision*, pp. 6833–6843, 2025.

550 Seokeon Choi, Debasmit Das, Sungha Choi, Seunghan Yang, Hyunsin Park, and Sungtrack Yun. Pro-  
 551 gressive random convolutions for single domain generalization. In *Proceedings of the IEEE/CVF  
 552 Conference on Computer Vision and Pattern Recognition*, pp. 10312–10322, 2023.

553 Yaroslav Ganin, Evgeniya Ustinova, Hana Ajakan, Pascal Germain, Hugo Larochelle, François  
 554 Laviolette, Mario March, and Victor Lempitsky. Domain-adversarial training of neural networks.  
*Journal of machine learning research*, 17(59):1–35, 2016.

555 Jintao Guo, Lei Qi, and Yinghuan Shi. Domaindrop: Suppressing domain-sensitive channels for  
 556 domain generalization. In *Proceedings of the IEEE/CVF international conference on computer  
 557 vision*, pp. 19114–19124, 2023a.

558 Jintao Guo, Na Wang, Lei Qi, and Yinghuan Shi. Aloft: A lightweight mlp-like architecture with  
 559 dynamic low-frequency transform for domain generalization. In *Proceedings of the IEEE/CVF  
 560 conference on computer vision and pattern recognition*, pp. 24132–24141, 2023b.

561 Wei Huang, Yilei Shi, Zhitong Xiong, and Xiao Xiang Zhu. Representation enhancement-  
 562 stabilization: Reducing bias-variance of domain generalization. In *European Conference on  
 563 Computer Vision*, pp. 108–125. Springer, 2025.

564 Muhammad Uzair Khattak, Hanoona Rasheed, Muhammad Maaz, Salman Khan, and Fahad Shah-  
 565 baz Khan. Maple: Multi-modal prompt learning. In *Proceedings of the IEEE/CVF conference on  
 566 computer vision and pattern recognition*, pp. 19113–19122, 2023.

567 David Krueger, Ethan Caballero, Joern-Henrik Jacobsen, Amy Zhang, Jonathan Binas, Dinghuai  
 568 Zhang, Remi Le Priol, and Aaron Courville. Out-of-distribution generalization via risk extrapo-  
 569 lation (rex). In *International conference on machine learning*, pp. 5815–5826. PMLR, 2021.

570 Da Li, Yongxin Yang, Yi-Zhe Song, and Timothy M Hospedales. Deeper, broader and artier domain  
 571 generalization. In *Proceedings of the IEEE international conference on computer vision*, pp.  
 572 5542–5550, 2017.

573 Da Li, Yongxin Yang, Yi-Zhe Song, and Timothy Hospedales. Learning to generalize: Meta-learning  
 574 for domain generalization. In *Proceedings of the AAAI conference on artificial intelligence*, vol-  
 575 ume 32, 2018a.

576 Junnan Li, Dongxu Li, Silvio Savarese, and Steven Hoi. Blip-2: Bootstrapping language-image  
 577 pre-training with frozen image encoders and large language models. In *International conference  
 578 on machine learning*, pp. 19730–19742. PMLR, 2023a.

579 Ming Li, Jike Zhong, Shitian Zhao, Yuxiang Lai, Haoquan Zhang, Wang Bill Zhu, and Kaipeng  
 580 Zhang. Think or not think: A study of explicit thinking in rule-based visual reinforcement fine-  
 581 tuning. *arXiv preprint arXiv:2503.16188*, 2025.

582 Ya Li, Mingming Gong, Xinmei Tian, Tongliang Liu, and Dacheng Tao. Domain generalization  
 583 via conditional invariant representations. In *Proceedings of the AAAI conference on artificial  
 584 intelligence*, volume 32, 2018b.

585 Ziyue Li, Kan Ren, Xinyang Jiang, Yifei Shen, Haipeng Zhang, and Dongsheng Li. Simple: Special-  
 586 ized model-sample matching for domain generalization. In *The Eleventh International Conference  
 587 on Learning Representations*, 2023b.

594 Haotian Liu, Chunyuan Li, Qingyang Wu, and Yong Jae Lee. Visual instruction tuning. *Advances*  
 595 *in neural information processing systems*, 36:34892–34916, 2023.  
 596

597 Yiran Luo, Joshua Feinglass, Tejas Gokhale, Kuan-Cheng Lee, Chitta Baral, and Yezhou Yang.  
 598 Grounding stylistic domain generalization with quantitative domain shift measures and synthetic  
 599 scene images. In *Proceedings of the IEEE/CVF Conference on Computer Vision and Pattern*  
 600 *Recognition*, pp. 7303–7313, 2024.

601 Subhransu Maji, Esa Rahtu, Juho Kannala, Matthew Blaschko, and Andrea Vedaldi. Fine-grained  
 602 visual classification of aircraft. *arXiv preprint arXiv:1306.5151*, 2013.  
 603

604 Hyeonseob Nam, HyunJae Lee, Jongchan Park, Wonjun Yoon, and Donggeun Yoo. Reducing do-  
 605 main gap by reducing style bias. In *Proceedings of the IEEE/CVF Conference on Computer Vision*  
 606 *and Pattern Recognition*, pp. 8690–8699, 2021.

607 OpenAI. Gpt-4 technical report. *arXiv preprint arXiv:2303.08774*, 2023.  
 608

609 Alec Radford, Jong Wook Kim, Chris Hallacy, Aditya Ramesh, Gabriel Goh, Sandhini Agar-  
 610 wal, Girish Sastry, Amanda Askell, Pamela Mishkin, Jack Clark, Gretchen Krueger, and Ilya  
 611 Sutskever. Learning transferable visual models from natural language supervision. pp. 8748–  
 612 8763, 2021a.  
 613

614 Alec Radford, Jong Wook Kim, Chris Hallacy, Aditya Ramesh, Gabriel Goh, Sandhini Agarwal,  
 615 Girish Sastry, Amanda Askell, Pamela Mishkin, et al. Learning transferable visual models from  
 616 natural language supervision. In *ICML*, 2021b.

617 Alexandre Rame, Corentin Dancette, and Matthieu Cord. Fishr: Invariant gradient variances for  
 618 out-of-distribution generalization. In *International Conference on Machine Learning*, pp. 18347–  
 619 18377. PMLR, 2022.

620 Shiori Sagawa, Pang Wei Koh, Tatsunori B Hashimoto, and Percy Liang. Distributionally robust  
 621 neural networks for group shifts: On the importance of regularization for worst-case generaliza-  
 622 tion. *arXiv preprint arXiv:1911.08731*, 2019.

623 Seungjae Shin, HeeSun Bae, Byeonghu Na, Yoon-Yeong Kim, and Il-chul Moon. Unknown domain  
 624 inconsistency minimization for domain generalization. In *The Twelfth International Conference*  
 625 *on Learning Representations*.

626 Andreas Steiner, André Susano Pinto, Michael Tschannen, Daniel Keysers, Xiao Wang, Yonatan  
 627 Bitton, Alexey Gritsenko, Matthias Minderer, Anthony Sherbondy, Shangbang Long, et al.  
 628 Paligemma 2: A family of versatile vlms for transfer. *arXiv preprint arXiv:2412.03555*, 2024.  
 629

630 Baochen Sun and Kate Saenko. Deep coral: Correlation alignment for deep domain adaptation. In  
 631 *European conference on computer vision*, pp. 443–450. Springer, 2016.

632 Quan Sun, Yuxin Fang, Ledell Wu, Xinlong Wang, and Yue Cao. Eva-clip: Improved training  
 633 techniques for clip at scale. *arXiv preprint arXiv:2303.15389*, 2023.  
 634

635 Gemini Team, Rohan Anil, Sebastian Borgeaud, Yonghui Wu, et al. Gemini: A family of highly  
 636 capable multimodal models. *arXiv preprint arXiv:2312.11805*, 2023.

637 Gemini Team, Petko Georgiev, Ving Ian Lei, Ryan Burnell, Libin Bai, Anmol Gulati, Garrett Tanzer,  
 638 Damien Vincent, Zhufeng Pan, Shibo Wang, et al. Gemini 1.5: Unlocking multimodal under-  
 639 standing across millions of tokens of context. *arXiv preprint arXiv:2403.05530*, 2024.  
 640

641 Vladimir Vapnik. *The nature of statistical learning theory*. Springer science & business media,  
 642 2013.

643 Hemanth Venkateswara, Jose Eusebio, Shayok Chakraborty, and Sethuraman Panchanathan. Deep  
 644 hashing network for unsupervised domain adaptation. In *Proceedings of the IEEE conference on*  
 645 *computer vision and pattern recognition*, pp. 5018–5027, 2017.

646 Pengfei Wang, Zhaoxiang Zhang, Zhen Lei, and Lei Zhang. Sharpness-aware gradient matching for  
 647 domain generalization. In *CVPR*, pp. 3769–3778, 2023.

648 Changsong Wen, Zelin Peng, Yu Huang, Xiaokang Yang, and Wei Shen. Domain generalization in  
 649 clip via learning with diverse text prompts. In *Proceedings of the Computer Vision and Pattern*  
 650 *Recognition Conference*, pp. 9559–9569, 2025.

651

652 Guowei Xu, Peng Jin, Ziang Wu, Hao Li, Yibing Song, Lichao Sun, and Li Yuan. Llava-cot: Let  
 653 vision language models reason step-by-step. *arXiv preprint arXiv:2411.10440*, 2024.

654

655 Zhipeng Xu, De Cheng, Xinyang Jiang, Nannan Wang, Dongsheng Li, and Xinbo Gao. Adversarial  
 656 domain prompt tuning and generation for single domain generalization. In *Proceedings of the*  
 657 *Computer Vision and Pattern Recognition Conference*, pp. 18584–18595, 2025.

658

659 Shen Yan, Huan Song, Nanxiang Li, Lincan Zou, and Liu Ren. Improve unsupervised domain  
 660 adaptation with mixup training. *arXiv preprint arXiv:2001.00677*, 2020.

661

662 Hantao Yao, Rui Zhang, and Changsheng Xu. Visual-language prompt tuning with knowledge-  
 663 guided context optimization. In *Proceedings of the IEEE/CVF conference on computer vision*  
 664 and pattern recognition, pp. 6757–6767, 2023.

665

666 Sangdoo Yun, Dongyoon Han, Seong Joon Oh, Sanghyuk Chun, Junsuk Choe, and Youngjoon Yoo.  
 667 Cutmix: Regularization strategy to train strong classifiers with localizable features. In *Proceed-  
 668 ings of the IEEE/CVF international conference on computer vision*, pp. 6023–6032, 2019.

669

670 Maxime Zanella and Ismail Ben Ayed. Low-rank few-shot adaptation of vision-language models.  
 671 In *Proceedings of the IEEE/CVF Conference on Computer Vision and Pattern Recognition*, pp.  
 672 1593–1603, 2024.

673

674 Hongyi Zhang, Moustapha Cisse, Yann N Dauphin, and David Lopez-Paz. mixup: Beyond empirical  
 675 risk minimization. In *International Conference on Learning Representations*, 2018.

676

677 Marvin Zhang, Henrik Marklund, Nikita Dhawan, Abhishek Gupta, Sergey Levine, and Chelsea  
 678 Finn. Adaptive risk minimization: Learning to adapt to domain shift. *Advances in Neural Infor-  
 679 mation Processing Systems*, 34:23664–23678, 2021.

680

681 Yuhui Zhang, Alyssa Unell, Xiaohan Wang, Dhruba Ghosh, Yuchang Su, Ludwig Schmidt, and  
 682 Serena Yeung-Levy. Why are visually-grounded language models bad at image classification?  
 683 *arXiv preprint arXiv:2405.18415*, 2024.

684

685 Kaiyang Zhou, Yongxin Yang, Yu Qiao, and Tao Xiang. Domain generalization with mixstyle. *arXiv  
 686 preprint arXiv:2104.02008*, 2021.

687

688 Kaiyang Zhou, Jingkang Yang, Chen Change Loy, and Ziwei Liu. Conditional prompt learning for  
 689 vision-language models. In *Proceedings of the IEEE/CVF conference on computer vision and*  
 690 *pattern recognition*, pp. 16816–16825, 2022a.

691

692 Kaiyang Zhou, Jingkang Yang, Chen Change Loy, and Ziwei Liu. Learning to prompt for vision-  
 693 language models. *International Journal of Computer Vision*, 130(9):2337–2348, 2022b.

694

695 Jinguo Zhu, Weiyun Wang, Zhe Chen, Zhaoyang Liu, Shenglong Ye, Lixin Gu, Hao Tian, Yuchen  
 696 Duan, Weijie Su, Jie Shao, et al. Internvl3: Exploring advanced training and test-time recipes for  
 697 open-source multimodal models. *arXiv preprint arXiv:2504.10479*, 2025.

698

699

700

701

A TRAINING PIPELINE FOR MCTC AND SARR MODULE

A.1 QUANTITATIVE VALIDATION OF REASONING CHAIN DOMAIN INVARIANCE

To verify the hypothesis that reasoning chains are more domain-invariant than visual features, we performed a quantitative validation. Following existing work that measures cross-domain distributional discrepancies (Guo et al., 2023b), we compute the Maximum Mean Discrepancy (MMD) between a source domain  $\hat{\mathcal{D}}_m^S = \{(\mathbf{x}_i, y_i)\}_{i=1}^{N_m^S}$  and a target domain  $\hat{\mathcal{D}}_{m'}^T = \{\mathbf{x}_j\}_{j=1}^{N_{m'}^T}$ . Let  $\mathbf{f}(\mathbf{x})$  denote the embedding extracted from CLIP’s vision encoder for visual features, or from CLIP’s

702  
 703 Table 3: Cross-domain divergence of visual embeddings and reasoning-chain embeddings for each  
 704 TerraInc class.

	bird	bobcat	cat	coyote	dog	empty	opossum	rabbit	raccoon	squirrel	Avg.
Domain divergence (Visual)	0.209	0.251	0.314	0.387	0.213	0.144	0.266	0.167	0.258	0.176	0.239
Domain divergence (Text)	0.054	0.048	0.103	0.114	0.093	0.126	0.091	0.103	0.142	0.115	0.099

708  
 709  
 710 text encoder for reasoning-chain embeddings. Under a linear kernel, MMD reduces to the squared  
 711 distance between mean embeddings:

$$713 \quad 714 \quad 715 \quad 716 \quad 717 \quad 718 \quad 719 \quad 720 \quad 721 \quad 722 \quad 723 \quad 724 \quad 725 \quad 726 \quad 727 \quad 728 \quad 729 \quad 730 \quad 731 \quad 732 \quad 733 \quad 734 \quad 735 \quad 736 \quad 737 \quad 738 \quad 739 \quad 740 \quad 741 \quad 742 \quad 743 \quad 744 \quad 745 \quad 746 \quad 747 \quad 748 \quad 749 \quad 750 \quad 751 \quad 752 \quad 753 \quad 754 \quad 755$$

$$\text{MMD}^2(\hat{\mathcal{D}}_m^S, \hat{\mathcal{D}}_{m'}^T) = \left\| \frac{1}{N_m^s} \sum_{i=1}^{N_m^s} \mathbf{f}(\mathbf{x}_i) - \frac{1}{N_{m'}^t} \sum_{j=1}^{N_{m'}^t} \mathbf{f}(\mathbf{x}_j) \right\|_2^2.$$

Using identical domain splits for both modalities, we compute the MMD for each category in TerraInc. As summarized in the Tab. 3, reasoning-chain embeddings exhibit dramatically lower cross-domain divergence than visual embeddings (average  $0.239 \rightarrow 0.099$ , a 58.6% reduction). This large gap provides clear quantitative evidence that reasoning chains capture semantically stable, class-relevant information that is far less sensitive to style, background, or environmental shifts than visual features. Therefore, the results strongly support our core hypothesis that reasoning chains are significantly more domain-invariant.

Table 4: Rejection rate across SARR iterations (N) on the four TerraInc domains.

	<b>L100</b>	<b>L38</b>	<b>L43</b>	<b>L38</b>	<b>Avg.</b>
N=0	41.78	39.25	40.84	36.18	39.51
N=1	21.66	22.14	17.56	15.57	19.23
N=2	18.49	17.98	15.07	13.64	16.30
N=3	17.07	15.74	14.43	12.01	14.81

## A.2 REJECTION RATE ANALYSIS IN SARR ITERATIONS

To quantify the filtering behavior of SARR, we measure the rejection rate, defined as the percentage of self-generated reasoning chains whose `<CONCLUSION>` does not match the ground-truth label. Using InternVL3-8B on the TerraInc dataset (see Tab. 4), we observe that the rejection rate is relatively high at  $N = 0$  (39.51%), reflecting the mismatch between GPT-4o-style reasoning and the model’s native prediction tendencies. After the first SARR iteration, the rejection rate drops sharply to 19.23%, and continues to decrease at  $N = 2$  and  $N = 3$ , eventually stabilizing around 15–17%.

This consistent downward trend indicates that, as SARR iterations progress, the model’s self-generated reasoning chains increasingly lead to correct conclusions. Rather than performing random filtering, SARR progressively strengthens the semantic alignment between the reasoning chain and the model’s final prediction. The improving correctness of self-generated chains demonstrates that the reasoning process itself becomes more stable, coherent, and predictive, providing direct evidence that RD-MLDG enhances reasoning quality rather than relying on incidental regularization effects.

## B RESULTS ON SMALLER OPEN-SOURCE MODEL

To evaluate whether MTCT and SARR can generalize to smaller open-source models without dedicated reasoning pretraining, we conducted additional experiments on LLaVA-1.5-7B, whose reasoning ability is substantially weaker than that of InternVL3. This is directly reflected in the reasoning-only baselines (see Tab. 5): under the same setting on TerraInc, InternVL3-2B achieves an average accuracy of 66.00%, whereas LLaVA-1.5-7B reaches only 62.07%, indicating a clear gap in their initial reasoning capability. Despite this weaker backbone, **our method remains consistently effective**. As shown in the table, MTCT improves LLaVA-1.5-7B from 62.07% to 63.92%, and adding

---

**756 Algorithm 1 RD-MLDG with MTCT and SARR**


---

757 **Require:** Source domains  $\{\hat{D}_m^S\}_{m=1}^{N_S}$ , base model  $f_\theta$ , DomainBed-Reasoning dataset, self-labeling rounds  $N$   
 758 **Ensure:** Fine-tuned model  $f_\theta$

760 **▷ Stage 1: Multi-Task Cross-Training (MTCT)**

761 1: **for** each minibatch  $\{(x_i, y_i, r_i)\}_{i=1}^B$  **do**  
 762 2: Construct classification prompt  $q_{\text{cls}}$  and reasoning prompt  $q_{\text{reason}}$   
 763 3: Compute classification loss  $L_{\text{cls}}$   
 764 4: Compute reasoning loss  $L_{\text{reason}}$   
 765 5: Update  $\theta$  with  $L_{\text{MTCT}} = L_{\text{cls}} + L_{\text{reason}}$  (Eq. 1)  
 766 6: **end for**

767 **▷ Stage 2: Self-Labeled Reasoning Regularization (SARR)**

768 7: **for**  $k = 1$  to  $N$  **do**  
 769 8: **for** each sample  $(x_i, y_i)$  **do**  
 770 9: Generate reasoning  $\hat{r}_i$  with  $q_{\text{reason}}$   
 771 10: Extract predicted conclusion between <CONCLUSION> and </CONCLUSION> tags  
 772 11: **if** conclusion =  $y_i$  **then**  
 773 12: Retain  $(x_i, y_i, \hat{r}_i)$  as supervision  
 774 13: **end if**  
 775 14: **end for**  
 776 15: Fine-tune on retained pairs with  $L_{\text{SARR}} = L_{\text{cls}} + L_{\text{reason}}$  (Eq. 2)  
 16: **end for**

---

777  
 778 Table 5: MTCT and SARR Performance on LLaVA-1.5 for TerraInc (%)  
 779

780 781 Idx	782 783 784 785 786 787 788 789 790 Method	791 792 793 794 795 796 797 798 799 TerraIncognita				
		796 L100	797 L38	798 L43	799 L46	799 Avg.
796 1	797 InternVL3-2B + Reasoning only (Baseline)	74.79	61.26	69.40	58.26	66.00
796 2	797 <b>InternVL3-2B + MTCT</b>	<b>77.82</b>	<b>65.03</b>	<b>72.71</b>	<b>59.41</b>	<b>68.74</b> ( $\uparrow 2.74\%p$ )
796 3	797 <b>InternVL3-2B + MTCT + SARR</b>	<b>82.43</b>	<b>66.54</b>	<b>73.62</b>	<b>61.15</b>	<b>70.94</b> ( $\uparrow 4.94\%p$ )
796 4	797 InternVL3-8B + Reasoning only	74.42	60.39	68.21	55.21	64.56
796 5	797 <b>InternVL3-8B + MTCT</b>	<b>76.78</b>	<b>60.55</b>	<b>71.94</b>	<b>59.47</b>	<b>67.19</b> ( $\uparrow 2.63\%p$ )
796 6	797 <b>InternVL3-8B + MTCT + SARR</b>	<b>81.74</b>	<b>66.12</b>	<b>73.38</b>	<b>61.36</b>	<b>70.65</b> ( $\uparrow 6.09\%p$ )
796 7	797 LLaVA-1.5-7B + Reasoning only (Baseline)	75.34	58.20	62.51	52.24	62.07
796 8	797 <b>LLaVA-1.5-7B + MTCT</b>	<b>79.87</b>	<b>58.93</b>	<b>63.38</b>	<b>53.48</b>	<b>63.92</b> ( $\uparrow 1.85\%p$ )
796 9	797 <b>LLaVA-1.5-7B + MTCT + SARR</b>	<b>80.93</b>	<b>60.01</b>	<b>64.51</b>	<b>55.14</b>	<b>65.15</b> ( $\uparrow 3.08\%p$ )

796 SARR further increases performance to 65.15%. A similar improvement is observed on InternVL3-  
 797 2B, indicating that both components provide stable gains even when the underlying model lacks  
 798 strong reasoning pretraining.

799 These results collectively demonstrate that RD-MLDG does not rely on a strong reasoning backbone.  
 800 **Both MTCT and SARR transfer effectively to smaller, weaker, and fully open-source multi-  
 801 modal models**, showing that the proposed framework is broadly applicable beyond large reasoning-  
 802 centric models.

803 **C RESULTS ON SINGLE DOMAIN GENERALIZATION**

804 **Background.** Most existing DG studies assume access to multiple source domains. However, in  
 805 practice, models are often required to generalize from a single source domain to multiple unseen  
 806 target domains (Single Domain Generalization, SDG). This setting is more challenging because the  
 807 model cannot rely on inter-domain variation during training, making reasoning supervision poten-  
 808 tially more valuable.

809 **Experiment Setting.** We conduct SDG experiments on the OfficeHome dataset, following the  
 810 standard protocol where one domain (Art, Clipart, Product, Real World) is used as the source do-

810  
 811 Table 6: SDG results (%) on OfficeHome. One domain is used as the source domain and the others  
 812 are used as the target domain. The best performances in comparisons are highlighted in **bold** and  
 813 the second-best ones are marked with underlines.

Method	Venue	A	C	P	R	Avg.
DANN (Ganin et al., 2016)	IJCAI'16	55.20	49.30	48.40	58.40	52.80
CORAL (Sun & Saenko, 2016)	ICCV'16	55.60	52.80	50.30	59.40	54.50
IRM (Arjovsky et al., 2019)	-	54.90	53.20	48.60	59.20	54.00
MMD (Li et al., 2018b)	ICCV'18	55.10	52.00	50.30	59.30	54.20
OrgMixup (Zhang et al., 2018)	ICLR'18	56.00	54.40	50.40	61.00	55.50
Mixup (Yan et al., 2020)	-	55.50	54.10	49.40	59.40	54.60
CutMix (Yun et al., 2019)	CVPR'19	53.50	52.20	47.70	60.20	53.40
CDANN (Ganin et al., 2016)	-	55.20	49.90	47.60	58.60	52.80
GroupDRO (Sagawa et al., 2019)	ICLR'20	55.10	52.00	50.30	59.30	54.20
MTL (Blanchard et al., 2021)	JMLR'21	55.30	53.30	49.00	60.40	54.50
ARM (Zhang et al., 2021)	NeurIPS'21	55.00	51.60	47.30	59.30	53.30
VREx (Krueger et al., 2021)	ICML'21	55.50	52.60	49.10	59.30	54.10
Mixstyle (Zhou et al., 2021)	ICLR'21	44.30	29.80	33.60	48.50	39.00
ERM (Vapnik, 2013)	ICLR'21	55.60	52.80	50.30	59.40	54.50
SAM (Li et al., 2018b)	ICLR'21	56.90	53.80	50.90	61.50	55.80
SagNet (Nam et al., 2021)	CVPR'21	56.90	53.40	50.80	61.20	55.60
FishR Rame et al. (2022)	ICML'22	55.10	51.20	49.20	59.90	53.90
RIDG (Chen et al., 2023b)	ICCV'23	56.80	55.40	50.50	60.90	55.90
SAGM (Wang et al., 2023)	CVPR'23	57.70	54.80	51.50	61.40	56.30
ITTA (Chen et al., 2023a)	CVPR'23	56.00	51.50	50.50	61.60	54.90
UDIM (Shin et al.)	ICLR'24	58.50	55.70	54.50	64.50	58.30
PAPT (Xu et al., 2025)	CVPR'25	<u>59.81</u>	<u>68.30</u>	<u>59.12</u>	60.87	62.03
<b>InternVL3-2B + RD-MLDG (Ours)</b>	-	<b>89.79</b>	<b>92.54</b>	<b>86.43</b>	<b>88.72</b>	<b>89.37</b>

833  
 834 main and the other three serve as target domains. We compare our method with representative  
 835 SDG approaches, including domain-invariant representation learning (IRM, CORAL, VREx), data  
 836 augmentation strategies (Mixup, CutMix, OrgMixup), adversarial learning (DANN, CDANN), and  
 837 recent single-domain adaptation methods (RIDG, SAGM, PAPT). For our approach, we evaluate  
 838 InternVL3-2B with RD-MLDG under the SDG setting.

839  
 840 **Observation.** As shown in Tab. 6, RD-MLDG achieves a large margin over all baselines, reaching  
 841 an average accuracy of 89.37%, compared to the best baseline PAPT at 62.03%. This indicates that  
 842 reasoning supervision, even from a single domain, provides strong class-relevant signals that transfer  
 843 effectively to unseen target domains. Notably, while prior methods rely on feature-level invariance  
 844 or adversarial strategies, our approach explicitly incorporates reasoning chains, which appear more  
 845 robust under severe domain shift.

846  
 847 Table 7: Base-to-new generalization results on FGVC-Aircraft.  
 848

Idx	Method	FGVC-Aircraft		
		Base	New	H
1	InternVL3-8B	20.35	17.83	19.01
2	+ Reasoning only (Baseline)	39.20	15.44	22.11
3	+ <b>MTCT</b>	<b>56.42</b>	<b>18.60</b>	<b>27.95</b> ( $\uparrow 5.84\%p$ )
4	+ <b>MTCT + SARR</b>	60.11	24.33	34.63( $\uparrow 12.52\%p$ )

855  
 856  
 857 D RESULTS ON BASE-TO-NEW EXPERIMENT

859  
 860 To evaluate the broader advantages of reasoning-driven domain generalization, we perform a base-  
 861 to-new class generalization experiment using the FGVC-Aircraft dataset (Maji et al., 2013).. Unlike  
 862 the appearance-based shifts seen in the DomainBed benchmarks, the base-to-new protocol intro-  
 863 duces semantic and compositional shifts within the label space. In this setting, the model must  
 864 transfer reasoning from familiar categories to structurally distinct, unseen ones. This task is more

864

865 Table 8: VQA and VE results (%) on VOLDOGER benchmark dataset. The best performances in  
866 comparisons are highlighted in **bold** and the second-best ones are marked with underlines.  
867

Method	VQA					VE				
	Real	Cartoon	Pencil	Oil	Avg.	Real	Cartoon	Pencil	Oil	Avg.
ViT	55.03	48.52	47.76	48.65	49.99	72.15	52.51	57.72	58.78	60.29
CLIP (Radford et al., 2021a)	58.23	49.11	50.41	49.41	51.79	73.10	55.85	61.61	60.93	62.87
BLIP (Li et al., 2023a)	59.19	50.29	51.32	50.88	52.92	66.73	48.26	52.93	53.62	55.39
<b>Open-Source Models.</b>										
BLIP2-FlanT5-XL (Li et al., 2023a)	65.29	64.41	61.18	62.92	63.45	63.82	73.13	72.24	72.00	70.30
PaliGemma (Steiner et al., 2024)	80.59	79.41	75.29	<u>75.59</u>	<u>77.72</u>	33.43	33.91	35.02	34.79	34.29
LLaVA-Next w/ Vicuna-7B (Liu et al., 2023)	80.29	67.65	64.12	64.12	69.93	55.76	55.25	57.95	55.18	56.03
LLaVA-Next w/ Mistral-7B (Liu et al., 2023)	81.76	65.88	61.18	64.41	68.31	70.05	70.36	67.86	69.24	69.38
<b>Proprietary Models.</b>										
GPT4-Vision 1106-preview (OpenAI, 2023)	75.29	67.06	59.12	62.35	65.96	65.32	70.59	70.51	71.20	69.41
GPT4-Turbo 2024-04-09 (OpenAI, 2023)	76.47	67.65	62.94	64.71	67.94	61.75	72.43	<u>72.58</u>	70.05	69.20
GPT4o 2024-05-13 (OpenAI, 2023)	<u>77.35</u>	<b>82.94</b>	<b>79.41</b>	<b>78.53</b>	<b>79.56</b>	71.08	73.13	72.47	70.74	<u>71.85</u>
Claude 3 Haiku	75.00	67.35	62.06	62.35	66.69	58.18	63.55	67.86	66.47	64.01
Claude 3 Sonnet	68.24	74.12	72.35	70.29	71.25	59.22	72.28	72.24	71.08	68.70
Claude 3 Opus	63.53	63.82	61.76	63.24	63.09	59.91	66.65	61.18	64.06	62.95
Gemini 1.0 Pro (Team et al., 2023)	73.23	68.24	68.23	68.82	69.63	64.63	60.32	63.13	64.29	63.09
Gemini 1.5 Flash (Team et al., 2024)	75.88	78.82	73.82	72.94	75.36	64.17	<b>74.39</b>	<b>73.96</b>	<b>72.35</b>	71.22
<b>RD-MLDG Method (Our).</b>										
LLaVA-1.5-7B (Zero shot)	0.29	0.59	0.29	0.29	0.37	0.23	0.12	0.23	0.23	0.20
LLaVA-1.5-7B + Reasoning only (Baseline)	75.88	59.41	59.71	59.71	63.68	67.51	66.32	67.28	67.35	67.12
LLaVA-1.5-7B + MTCT	78.53	68.82	64.71	65.59	69.41	72.35	65.97	67.74	66.24	68.08
LLaVA-1.5-7B + MTCT + SARR	80.88	71.17	67.06	67.35	71.62	73.96	69.12	68.89	68.54	70.13
InternVL3-2B (Zero shot)	0.59	0.29	0.29	0.59	0.44	0.34	0.23	0.34	0.34	0.31
InternVL3-2B + Reasoning only (Baseline)	74.12	66.76	66.18	63.82	67.72	67.97	63.67	65.55	67.17	66.09
InternVL3-2B + MTCT	83.53	69.41	68.53	69.12	72.65	71.20	65.05	66.94	66.71	67.48
InternVL3-2B + MTCT + SARR	85.29	71.47	69.71	71.17	74.41	<u>74.30</u>	68.20	69.35	68.66	70.13
InternVL3-8B (Zero shot)	81.76	69.12	69.71	68.24	72.21	70.85	62.28	65.90	64.86	65.97
InternVL3-8B + Reasoning only (Baseline)	81.47	74.12	70.88	67.94	73.60	73.50	70.13	68.32	70.39	70.59
InternVL3-8B + MTCT	83.82	77.94	71.47	68.53	75.44	73.96	68.54	69.35	71.57	70.62
InternVL3-8B + MTCT + SARR	<b>85.00</b>	<u>81.76</u>	72.94	69.41	77.28	<b>74.76</b>	70.85	70.62	<u>72.11</u>	<b>72.09</b>

888

889 challenging than traditional domain shifts as it requires the model to handle shifts in the underlying  
890 category structure rather than just appearance.  
891892 The FGVC-Aircraft dataset is particularly well-suited for this evaluation because its categories are  
893 defined by fine-grained structural and compositional attributes, such as wing geometry and engine  
894 configuration. These attributes make the task heavily reliant on structured reasoning rather than  
895 surface-level visual cues, providing an ideal benchmark to test the model’s ability to generalize  
896 through reasoning across different domains.  
897898 **Experiment setting:** Concretely, following existing work (Zhou et al., 2022b) that adopts the widely  
899 used base-to-new evaluation setting, we randomly split the 100 aircraft categories into 50 base and  
900 50 new classes. All models are trained only on the base classes, and at test time we evaluate them  
901 on both base and unseen new classes, reporting performance on each split as well as their harmonic  
902 mean  $H$ . This setting ensures that good performance requires not only retaining accuracy on seen  
903 categories, but also transferring learned reasoning to semantically novel and compositionally distinct  
904 categories, thereby creating a genuine conceptual generalization scenario.  
905906 **Observation:** As shown in the Tab. 7, RD-MLDG improves harmonic mean accuracy from 19.01%  
907 → 34.63%, representing a substantial gain under this challenging conceptual shift. Notably, accuracy  
908 on unseen new classes increases from 15.44% → 24.33%, demonstrating that reasoning super-  
909 vision enhances transfer to semantically novel and compositionally distinct categories rather than  
910 merely improving robustness to stylistic or appearance-level variations. These results provide direct  
911 empirical evidence that **RD-MLDG benefits conceptual generalization beyond the appearance-  
912 level shifts captured by existing benchmarks.**  
913914 

## E EXPLORING THE EFFECTIVENESS OF RD-MLDG ON VQA AND VE 915 (VISUAL ENTAILMENT)

916 **RD-MLDG is designed to be flexible and adaptable across various tasks.** Both MTCT and  
917 SARR are built on structured reasoning-chain supervision, making the framework task-agnostic.  
918 This means that as long as a task follows a general “vision → reasoning → output” pathway, RD-  
919

918 MLDG can be seamlessly applied without requiring changes to the model architecture or the opti-  
 919 mization process.

920 In the Sec. 3, we adopt the DomainBed setting because it is the most widely used and standardized  
 921 benchmark for studying domain generalization. Building on this foundation allows us to investigate  
 922 reasoning-chain supervision within a well-established DG framework, ensuring that our analysis  
 923 of the challenges introduced by reasoning in DG is performed under consistent and community-  
 924 recognized evaluation conditions. Through this setting, we identify and study two fundamental  
 925 challenges caused by reasoning in DG: (i) the optimization difficulty and high-entropy gradients  
 926 (Sec. 4.1), and (ii) the reasoning-pattern mismatch between external LLMs and target multimodal  
 927 models (Sec. 4.2). MTCT and SARR are explicitly designed to address these two issues, and their  
 928 mechanisms are independent of the specific downstream task used to study them.

929 **Extension to VQA and VE:** To verify the task generality of RD-MLDG beyond visual classi-  
 930 fication, we extend our method to two multimodal tasks: VQA and Visual Entailment (VE). We  
 931 construct reasoning-augmented versions of both VOLDOGER-VQA and VOLDOGER-VE (Choi  
 932 et al., 2025) so that their data formats align with DomainBed-Reasoning. Each sample is aug-  
 933 mented with the same five structured components: <SUMMARY>, <CAPTION>, <REASONING>,  
 934 <REFLECTION>, and <CONCLUSION>. This ensures that both MTCT and SARR can be applied  
 935 without architectural changes to any model. Both datasets contain four visually heterogeneous do-  
 936 mains (Real, Cartoon, Pencil, Oil). The style shifts significantly affect visual perception, textual  
 937 grounding, and multimodal alignment. This makes VQA and VE natural testbeds for assessing  
 938 whether reasoning-driven DG generalizes beyond classification.

939 **Observation:** Across both the VQA and VE tasks, our results (see Tab. 8) consistently demonstrate  
 940 that RD-MLDG extends well beyond visual classification and remains effective in multimodal set-  
 941 tings that require joint visual grounding and reasoning. On the VQA task, InternVL3-8B improves  
 942 from 73.60% (reasoning-only baseline) to 75.44% with MTCT and further to 77.28% with SARR.  
 943 On the VE task, the same model improves from 70.59% to 70.62% and finally to 72.09% after apply-  
 944 ing both modules. These gains are not isolated to a single model: LLaVA-1.5-7B, which lacks any  
 945 reasoning-oriented pretraining, shows even larger improvements, rising from 63.68% → 69.41% →  
 946 71.62% on VQA and from 67.12% → 68.08% → 70.13% on VE. InternVL3-2B exhibits a similar  
 947 trend on both tasks.

948 Beyond absolute gains, RD-MLDG also enhances the competitiveness of the underlying models  
 949 relative to stronger multimodal LLMs. After applying MTCT and SARR, InternVL3-8B surpasses  
 950 most zero-shot MLLMs, including BLIP2, the Claude 3 family, Gemini 1.0 and 1.5, and several  
 951 LLaVA-Next variants, in average accuracy across all four visual styles for both VQA and VE. The  
 952 fact that these improvements appear consistently across two distinct multimodal tasks, each involv-  
 953 ing substantial style-induced domain shifts (Real, Cartoon, Pencil, Oil), further confirms that MTCT  
 954 and SARR enable the model to learn domain-invariant reasoning patterns that remain stable across  
 955 different cross-modal decision-making objectives.

956 Taken together, the consistent performance gains across VQA and VE, coupled with improvements  
 957 over a large set of open-source and proprietary multimodal baselines, provide strong evidence that  
 958 RD-MLDG is a task-agnostic and broadly applicable reasoning-driven DG framework. The results  
 959 confirm that our approach enhances the robustness and domain invariance of reasoning chains in  
 960 diverse multimodal environments, thereby validating its generality far beyond visual classification.

## 961 F LARGE LANGUAGE MODEL USAGE STATEMENT

963 We relied on a large language model (LLM) only for language refinement (grammar, wording, and  
 964 clarity). The LLM did not contribute to the conception of ideas, study design, data collection,  
 965 analysis, or figure/table generation, and it did not write technical content. All methodological and  
 966 experimental contributions, as well as the interpretation of results and final decisions, are by the  
 967 authors.

972

973

974

975

976

**Instruct prompt:**

I have an image and a question that I want you to answer. I need you to strictly follow the format with five specific sections: SUMMARY, CAPTION, REASONING, REFLECTION, and CONCLUSION. It is crucial that you adhere to this structure exactly as outlined and that the final answer in the CONCLUSION matches the standard correct answer precisely. To explain further: In SUMMARY, briefly explain what steps you'll take to solve the problem. In CAPTION, describe the contents of the image, specifically focusing on details relevant to the question. In REASONING, outline a step-by-step thought process you would use to solve the problem based on the image. In REFLECTION, critically assess your reasoning, considering potential ambiguities, alternative interpretations, or justifying why your logic is most sound. In CONCLUSION, give the final answer in a direct format, and it must match the correct answer exactly. If it's a multiple choice question, the conclusion should only include the option without repeating what the option is. Here's how the format should look: <SUMMARY>[Summarize how you will approach the problem and explain the steps you will take to reach the answer.] </SUMMARY> <CAPTION>[Provide a detailed description of the image, particularly emphasizing the aspects related to the question.] </CAPTION> <REASONING>[Provide a chain-of-thought, logical explanation of the problem. This should outline step-by-step reasoning.] </REASONING> <REFLECTION>[Review and evaluate your reasoning. Consider any uncertainties or edge cases, and reaffirm why the answer is reliable.] </REFLECTION> <CONCLUSION>[State the final answer in a clear and direct format. It must match the correct answer exactly.] </CONCLUSION>(Do not forget </CONCLUSION>!) Please apply this updated format meticulously to analyze the given image and answer the related question, ensuring that the answer matches the standard one perfectly.

**Question prompt:**

Question: Please describe the category of the image. I will provide a series of options, each separated by a comma.

Options: ['bird', 'bobcat', 'cat', 'coyote', 'dog', 'empty', 'opossum', 'rabbit', 'raccoon', 'squirrel']

1018

1019

Figure 8: Input prompt template used for reasoning-chain generation. The prompt consists of two parts: (i) a question instruction paired with an image and candidate label options, and (ii) explicit guidelines requiring the model (GPT-4o) to output reasoning in a structured five-section format (SUMMARY, CAPTION, REASONING, REFLECTION, CONCLUSION). These generated reasoning chains are then paired with ground-truth labels and used to fine-tune downstream multimodal LLMs.

1024

1025